

15205      REGOLITH BRECCIA, GLASS-COATED      ST. 2      337.3 g

INTRODUCTION: 15205 has the characteristics of a breccia formed from an exceptionally immature regolith, but is unique among Apollo 15 regolith samples: it is gray, not brown, is tough, and consists almost entirely of Apollo 15 KREEP basalt fragments with some mare basalt fragments (especially pyroxene-phyric). While it contains green glass as clods and impact glasses, mature regolith components such as agglutinates are rare to absent, and the clast size is much larger than for mature regoliths (Fig. 1). The finest matrix appears to be glass and tiny mineral and lithic fragments. The rock has a distinct fabric.



Fig. 1a



Fig. 1b

Figure 1. Macroscopic views of 15205.

- a) freshly broken interior piece showing large pale lithic clasts, fractures, and blocky nature. S-71-46350;
- b) opposite view from a), showing exposed vesicular, planar glass. S-71-46341;
- c) close up of fractured face of ,0, showing large KREEP basalt clasts, solid matrix, and pieces chipped off. S-77-22162

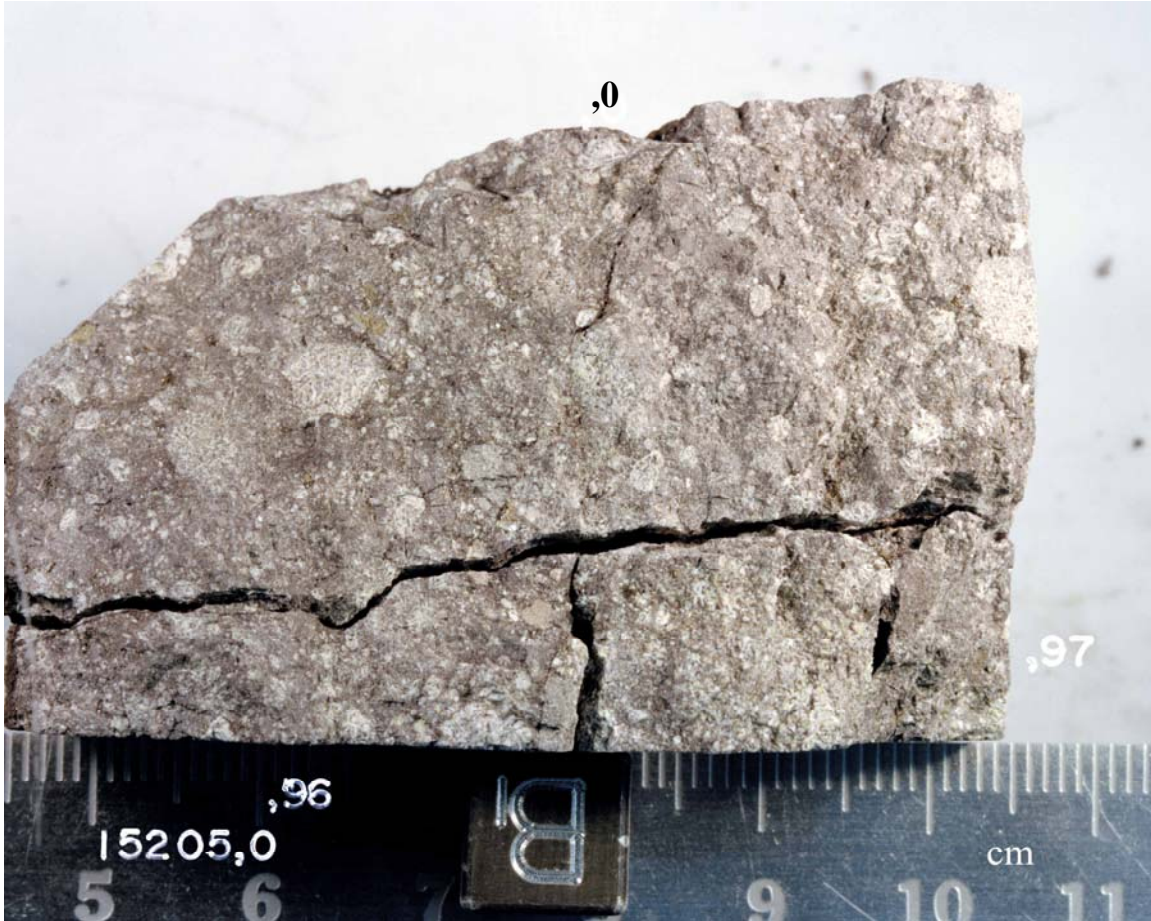


Fig. 1c

Glass coats most surfaces (Fig. 1) and is vesicular. These surfaces were not all exposed on the Moon and the glass surfaces penetrated a fracture system in the host boulder. The rock is angular with orthogonal joints and more than one penetrative fracture system. Zap pits are present on several surfaces, with most on one surface.

15205 was chipped from a boulder at St. 2 (Fig. 2 and Fig. 15105-2); 15206 was chipped from the same boulder. The boulder is anomalously large for the area and appears to have been thrown in less than 1 m.y. ago from the north or north-west and rolled to the southern end of its own crater.

PETROLOGY: 15205 is a tough breccia with light-colored basaltic lithic clasts (KREEP basalt) dominant (Fig. 1c). It was described by Dymek et al. (1974) as a regolith breccia, but it is not similar to other Apollo 15 regolith breccias: it has a  $I_s/FeO$  of 0 (McKay et al., 1984). According to McKay and Wentworth (1983) it has little intergranular porosity, agglutinates and glass spheres are rare, but shock features are common. Nagle (1982a) found that 15205 had lineation and other characteristics expected for rocks produced by subcrater lithification. Nagle (1982b) tabulated grain size distribution, rounding, and packing data for one thin section.

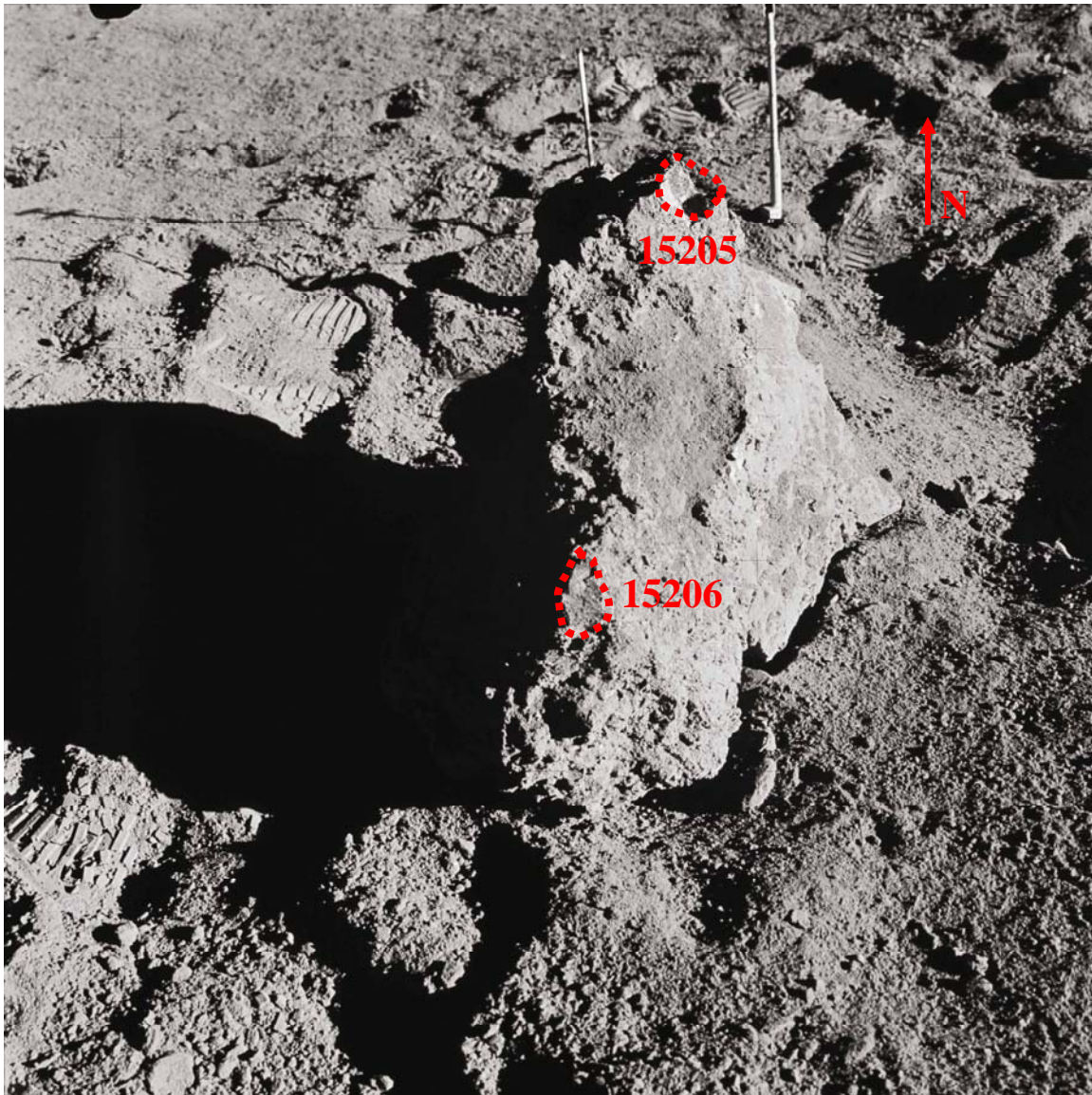


Figure 2. Locations of 15205 and 15206 on the boulder from which they were taken, post-sampling, pre-turning-over of the boulder. AS-15-86-11559

Dymek et al. (1974) concluded that 15205 was a layered, lithified regolith breccia. They described most of its characteristics as inferred from macroscopic descriptions and inspection of a series of thin sections (see Fig. 13). They found it to consist of about 75% clasts (~40% lithic, ~15% glass, and ~20% mineral fragments) from 10 microns to 1 cm diameter, set in a finer-grained, clastic matrix of glass and mineral particles (Fig. 3). Reaction between clasts and matrix is not present, and much of the glass shows no devitrification. Takeda et al. (1980) found a similar matrix. They noted that most pyroxene fragments are derived from KREEP basalts, and that none contain exsolution lamellae. Lithic clasts exhibit a wide range of granulation and shock effects which preceded accumulation. Dymek et al. (1974) also found a distinct fabric marked by a consistent alignment of clasts in thin section.

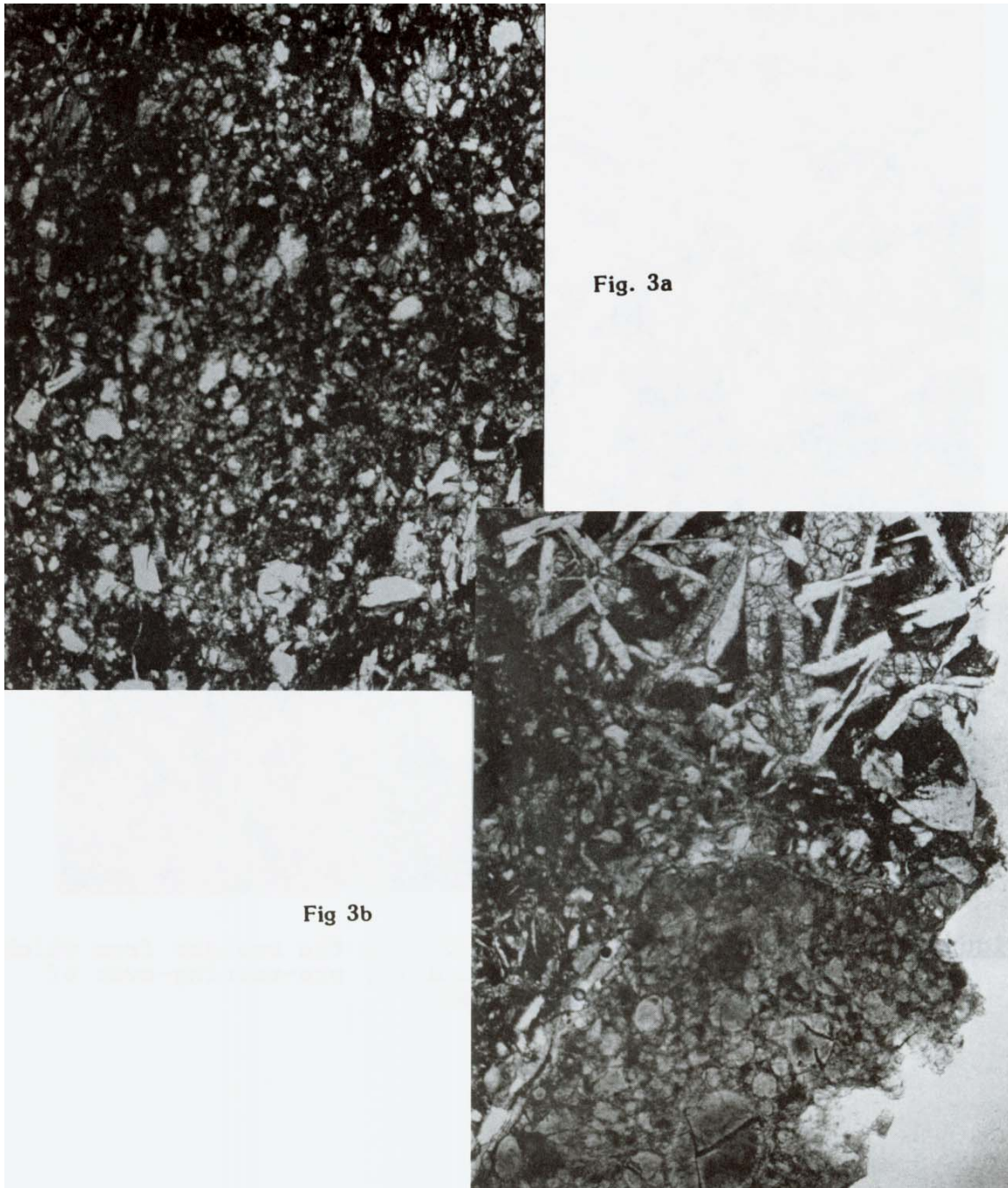
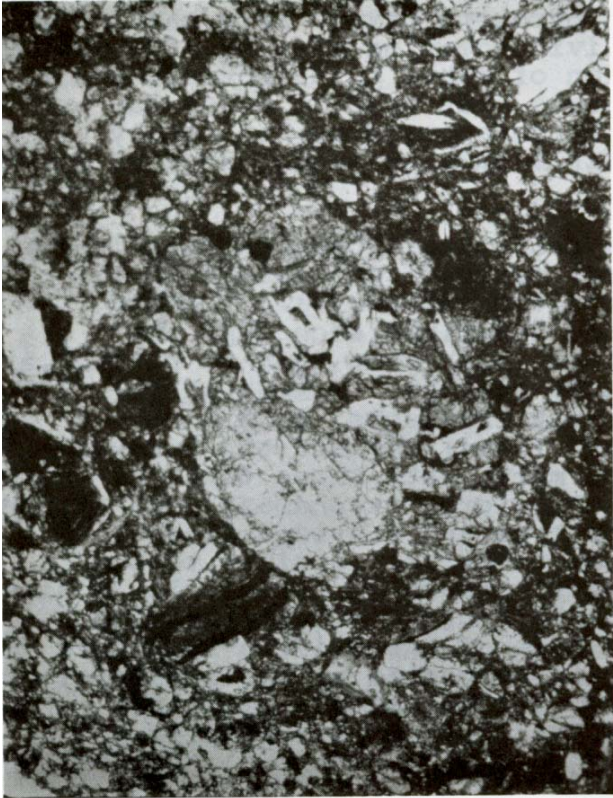
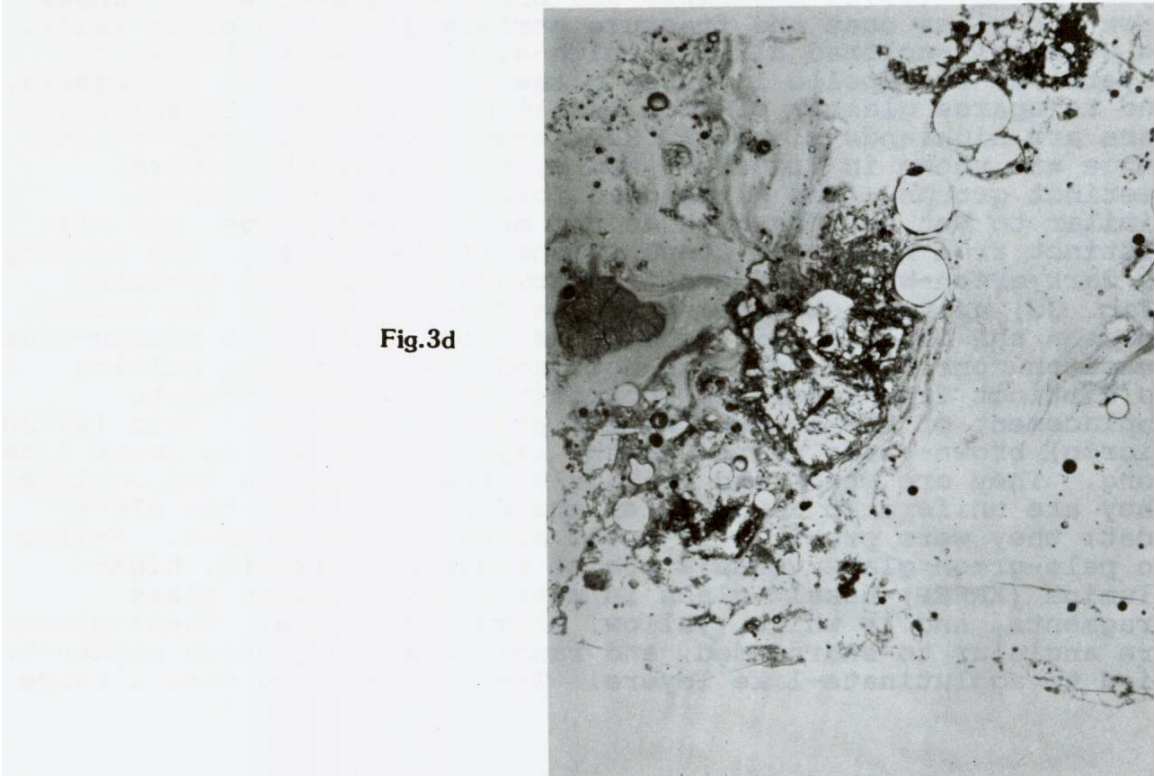


Figure 3. Photomicrographs of 15205. All transmitted light, widths about 1.25 mm.

- a) 15205,4. general matrix view showing predominance of material larger than 10 microns;
- b) 15205,4. clast of KREEP basalt (top) and brown, perlitic brown glass with vesicular rind;
- c) 15205,4. matrix and small clast of mare(?) basalt of uncertain affinity;
- d) 15205,110. glass coat, vesicular, banded, and with inclusions.



**Fig. 3c**



**Fig.3d**

Dymek et al. (1974) found that Apollo 15 KREEP basalt clasts make up about 20% of the sample, and pyroxene-phyric mare basalts a similar amount, while other, olivine-bearing mare basalts make up about 1% of the rock. Inspection of other thin sections and the bulk chemistry of the rock suggests that overall 15205 may contain much less mare basalt (which appears to be locally concentrated) and much more KREEP basalt than suggested by Dymek et al. (1974).

Dymek et al. (1974) divided the feldspathic basalts (Apollo 15 KREEP basalts) into five textural groups: subophitic to intersertal, intersertal, porphyritic intersertal, "ladder structure," and variolitic. They described each type and provided mineral analyses (Fig. 4) which show them to be similar to other described Apollo 15 KREEP basalts. Takeda et al. (1980) also briefly described KREEP basalt fragments, with mineral compositions given. Dymek et al. (1974) divided the pyroxenophytic basalts (quartz-normative mare) into three textural groups: aphanitic groundmass; ~10 micron groundmass; ~25 micron groundmass. They described each type and provided mineral analyses (Fig. 5) which show them to be very similar to the typical pyroxene-phyric mare basalts found at the Apollo 15 site. The few other mare basalt fragments include olivine-bearing varieties and may be similar to some of the olivine-normative mare basalts found at the site, as suggested by their mineral compositions (Fig. 6). Conspicuously absent are highlands lithologies; a few fragments of "moderately recrystallized metaclastic rock" are present.

Dymek et al. (1974) described and analyzed glass, which ranges from the glass coat and fracture surface glass, to brown veins, to variously-colored alkalic, high-alumina basalt glasses and layers, to the Apollo 15 green glass which exists as aggregates, and to sparse glasses of mare basalt composition. Conspicuously rare are highlands glasses. Some examples of the compositional range are shown in Figures 7 and 8, which show the several distinct groups. The glass coat forms a distinct cluster, similar to but not the same as the brown glass veins, and also distinct from bulk rock compositions (Tables 1, 2). The coating is dark green-brown and contains abundant spherical vesicles (Fig. 3d) up to 1 cm across. It is flow-banded and the contact between the breccia and the coat is sharp with a 100 micron-wide reaction zone. The coat was not produced by in situ melting. It is distinct from local soil compositions and must predate emplacement of the boulder at its present location. Thin (50-200 micron) brown-glass veins cut the layering and are at least 2 cm long. They are sharp and contain mineral particles and vesicles. They are uniform in composition and different from the glass coat; they were probably injected along microfractures. Yellow to pale-green glass veins are also present. Alkalic, high alumina (KREEP) basalt glass is most abundant among glass fragments, and is white, yellow, brown, or purple. These glasses are angular to subrounded, and range from homogeneous nondevitrified to agglutinate-like layers. The compositions show a range distinct from other glass types and their average is similar to that of Apollo 15 KREEP basalts. Green-glass fragments are spheres or sphere fragments, occurring singly and in aggregates, and are the common Apollo 15 volcanic glass (Table I) and include devitrified varieties. A few contain vesicles; a few contain euhedral phenocrysts (F<sub>079-82</sub>) similar to the experimentally determined liquidus composition. The chemical variation of clear green glasses is outside of analytical error and consistent with removal of about 5% liquidus olivine. Glass in partly crystallized spheres including that with olivine

15205 - FELDSPATHIC BASALT GROUP

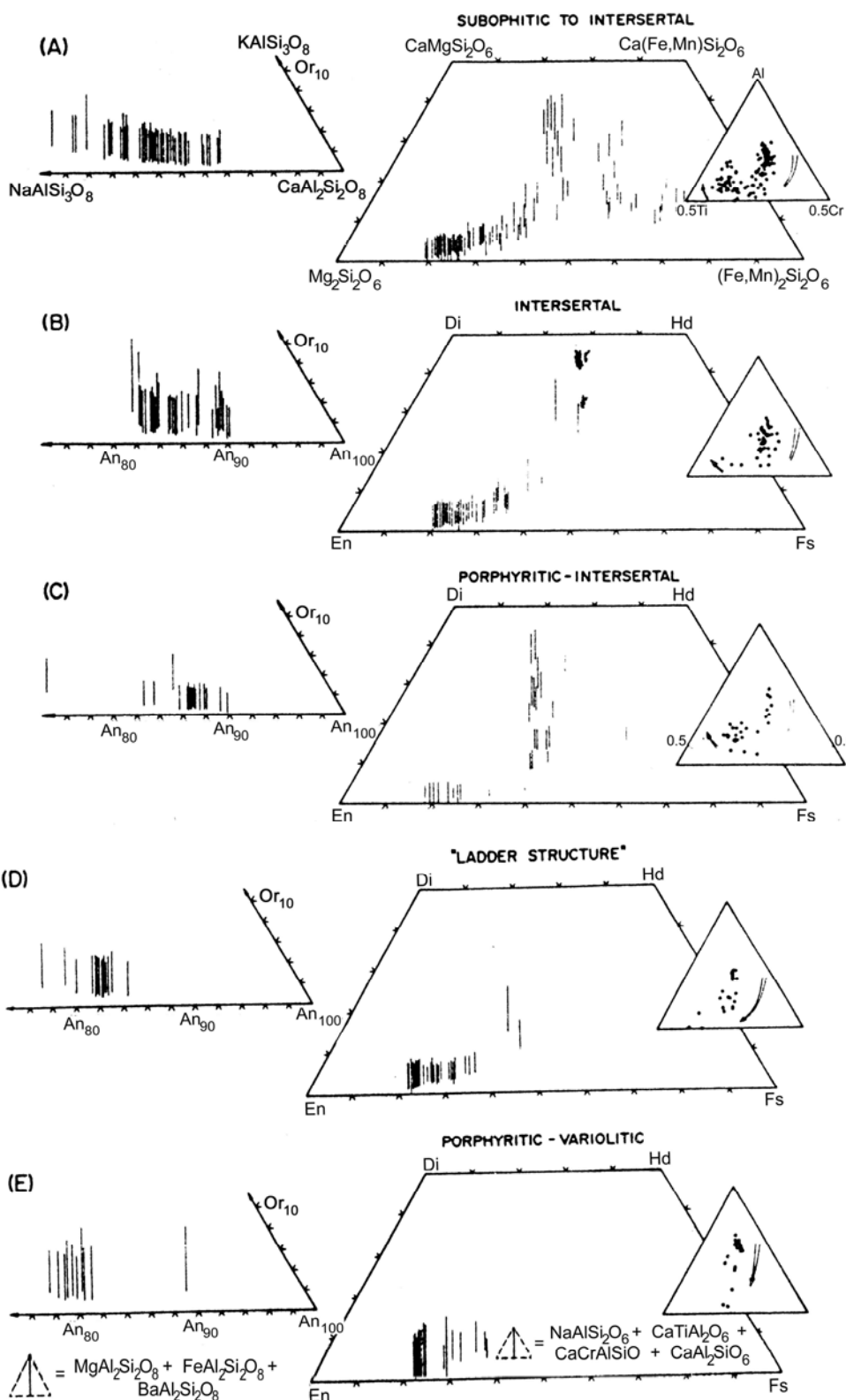


Figure 4. Compositions of plagioclases and pyroxenes in KREEP basalt clasts (Dymek et al., 1974).

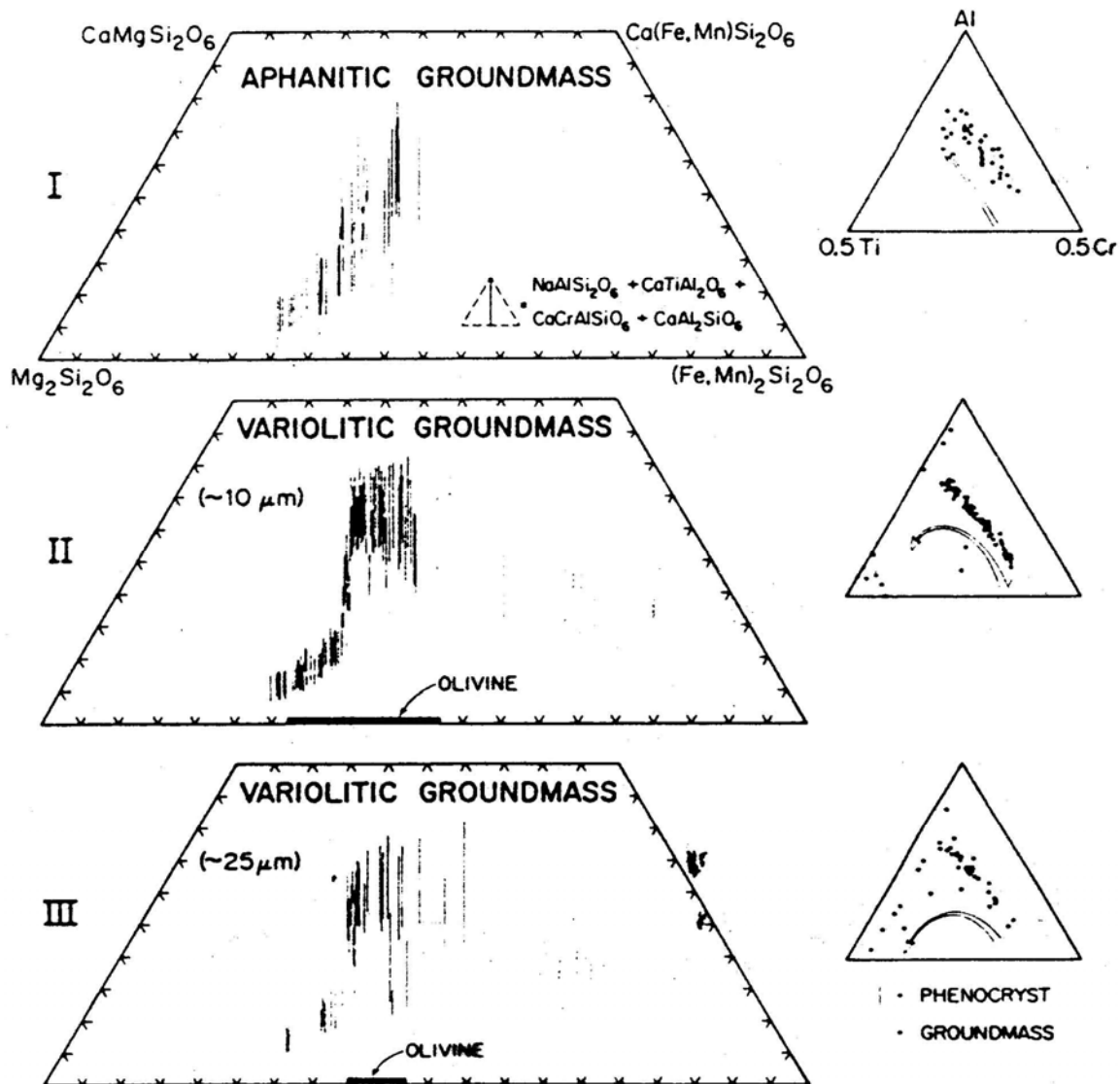


Figure 5. Compositions of pyroxene-phyric (quartz-normative) basalt clasts (Dymek et al., 1974).

phenocrysts is more evolved, suggesting that the phenocrysts do not reflect processes occurring during ascent and eruption. The green glass aggregates occur as clasts (clods) up to 1 cm long; the matrix of the clods is also green glass. The green glass clods also contain a few fragments of plagioclase, pyroxene, and pyroxene-phyric basalt. Glass with mare basalt compositions occurs as bright yellow to orange fragments (and as melts at the edge of mare basalt clasts) but are rare. A single angular white fragment with the composition of gabbroic anorthosite was identified, and rare plagioclase glass ( $An_{81-88}$ ) is present.

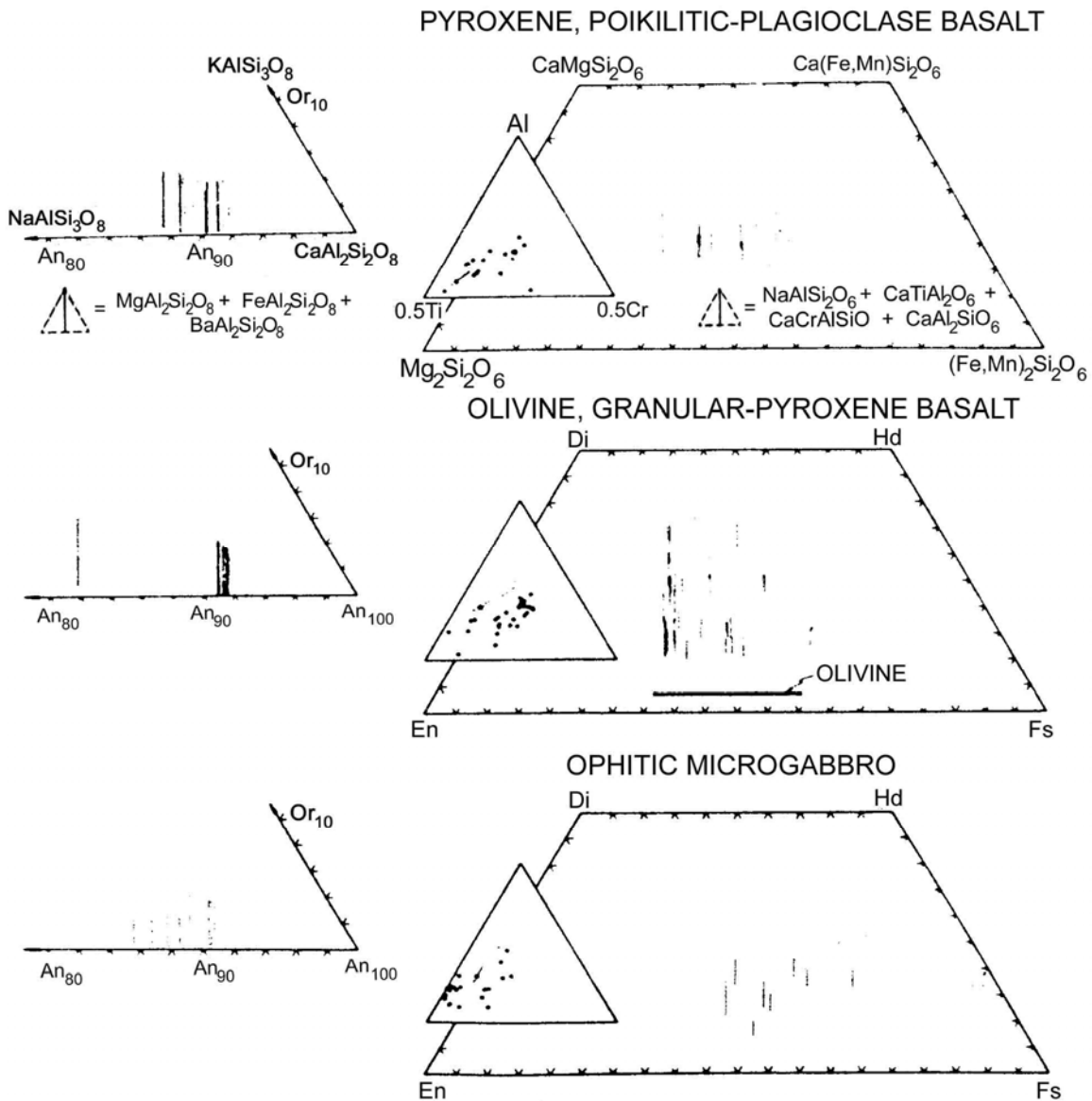


Figure 6. Compositions of plagioclases and pyroxenes in mare basalt clasts in 15205 (Dymek et al., 1974).

Both glass and lithic fragments suggest that a typical highland region was not an important contributor to the 15205 "soil." Dymek et al. (1974) concluded that feldspathic basalt (KREEP) fragments and glass equivalents together compose about 30% of sample 15205; in light of other observations and the bulk rock chemistry it is likely that the percentage is considerably higher.

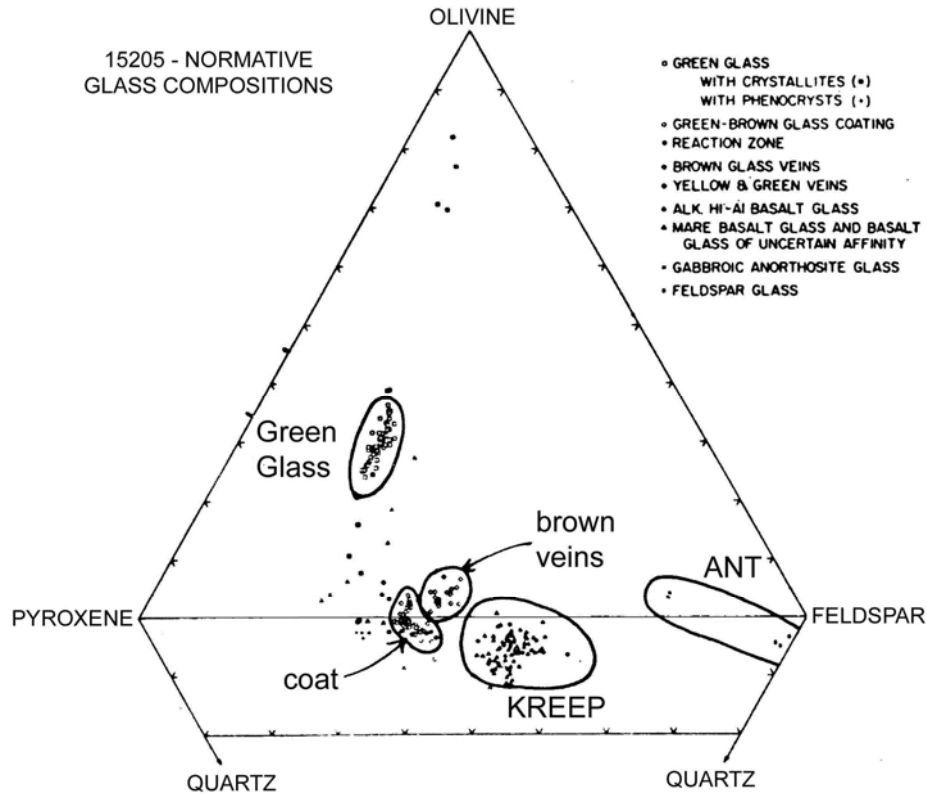


Figure 7. Compositions of glasses in 15205 on catatom ol-px-feldspar-qz diagram (Dymek et al., 1974).

TABLE 15205-1. Part of glass data of Dymek et al. (1974)  
(see original for minor element data and ranges)

	1	2	3	4	5	6	7	8
SiO <sub>2</sub>	48.4	47.3	47.5	51.4	45.6	50.5	44.6	47.7
TiO <sub>2</sub>	1.82	1.60	1.49	1.94	0.43	1.77	0.23	1.67
Al <sub>2</sub> O <sub>3</sub>	12.6	14.2	10.9	15.9	7.4	16.3	27.4	9.4
FeO	15.1	14.1	17.0	10.4	19.6	9.6	4.5	20.1
MgO	10.3	10.3	10.9	7.7	17.5	8.3	4.8	9.8
CaO	9.9	10.8	10.1	10.2	8.3	10.5	16.6	10.4
Na <sub>2</sub> O	0.54	0.50	0.47	0.88	0.15	0.77	0.24	0.36
K <sub>2</sub> O	0.25	0.22	0.13	0.52	0.02	0.61	0.03	0.07
P <sub>2</sub> O <sub>5</sub>	0.25	0.24	0.15	0.56	0.03	0.52	0.05	0.06
Cr ppm	3000	2600	3100	900	3800	1800	750	3000
Mn ppm	1600	1400	1800	700	2100	1100	1600	1200

### References for Table 15205-2

#### References and methods:

- (1) Keith et al. (1972); gamma ray spectroscopy
- (2) Rancitelli et al. (1972); gamma ray spectroscopy
- (3) Willis et al. (1972); XRF
- (4) Korotev (1984 unpublished); INAA
- (5) Allen et al. (1973); leach and INAA
- (6) Baedeker et al. (1973); INAA
- (7) Reed and Jovanovic (1972); NAA
- (8) Moore et al. (1973); combustion, gas chromatography

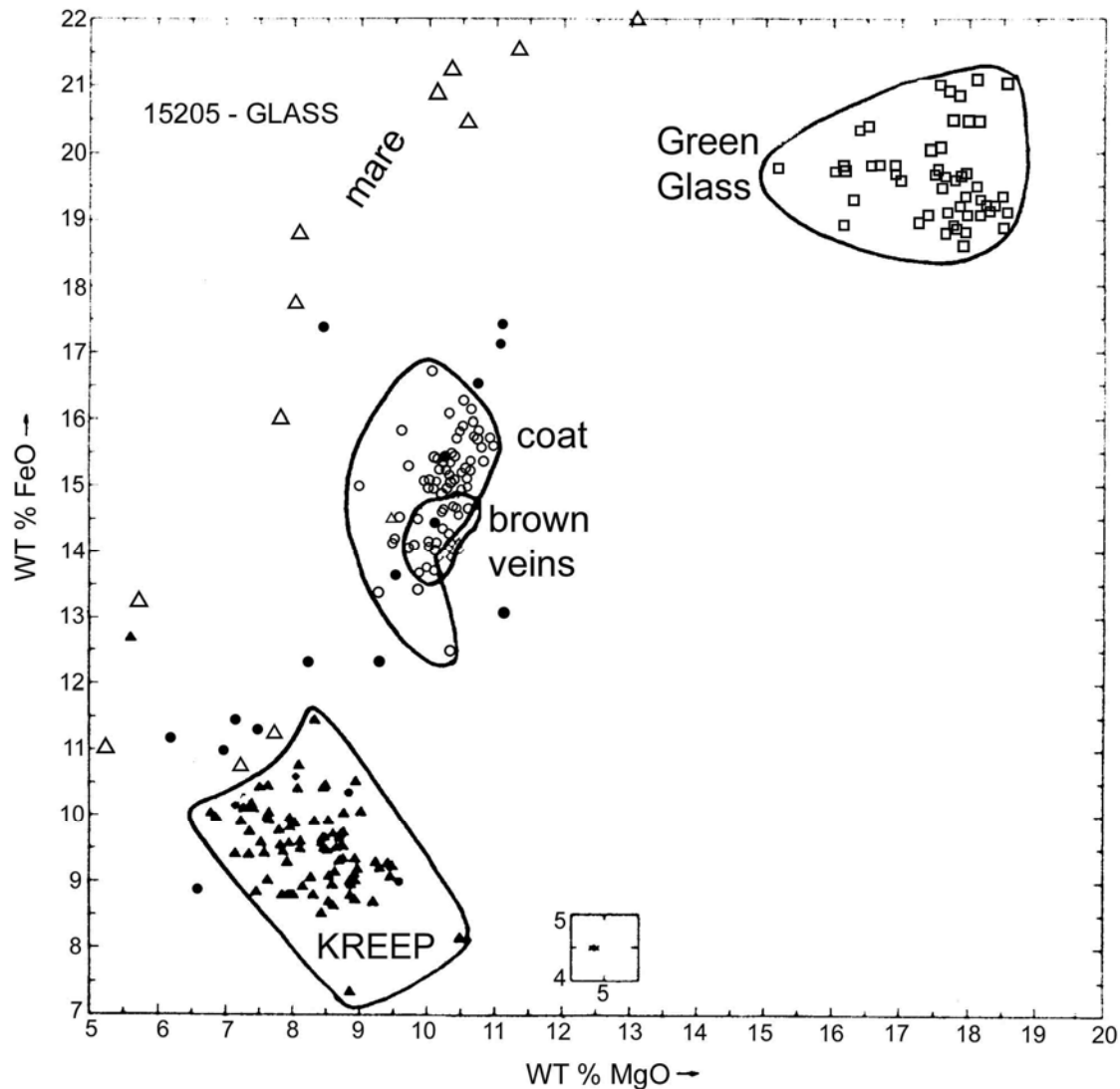


Figure 8. Compositions of glasses in 15205 on FeO vs. MgO diagram; symbols as in Figure 7 (Dymek et al., 1974).

Wilshire and Moore (1974) briefly discussed the planar glass on 15205. The glass veneers orthogonal fracture surfaces, are quite thin, and have thin spokes projecting out of the rock surface. The spikes suggest that the boulder was separated from a larger rock mass, which was cut by the orthogonal fractures, while the glass was still molten.

**CHEMISTRY:** Analyses of bulk material of 15205 are listed in Table 2. The rare earths are plotted in Figure 9. Most analyses seem to be of nearly pure Apollo 15 KREEP basalt; that of Korotev (1984 unpublished) contains more mare component. The coarse size of the clasts and heterogeneous nature of the population distribution suggest that considerable sampling problems could arise for bulk rock analyses, especially for small

TABLE 15205-2. Bulk rock chemical analyses

	,0(a)	,0	,37	,114	,35	,38	,35	,32
wt %								
SiO <sub>2</sub>			51.03					
TiO <sub>2</sub>			1.99					
Al <sub>2</sub> O <sub>3</sub>			14.92					
FeO			11.28	13.3				
MgO			8.23					
CaO			9.94	8.9				
Na <sub>2</sub> O			0.73	0.66				
K <sub>2</sub> O	0.528	0.562	0.528					
P <sub>2</sub> O <sub>5</sub>			0.557					
(ppm)								
Sc				28.5				
V								
Cr			2330	2770				
Mn			1232					
Co				30.2				
Ni				59		28		
Rb			14.4					
Sr			171	150				
Y			201					
Zr			979	710				
Nb			59.4					
Hf				18.5				
Ba			673	500				
Th	12.0	12.6		8.0				
U	2.9	3.28		2.2			3.2	
Pb								
La				49.6				
Ce				131				
Pr								
Nd				76				
Sm				22.8				
Eu				2.02				
Gd								
Tb				4.54				
Dy								
Ho								
Er								
Tm								
Yb				15.5				
Lu				2.16				
Li							22	
Be								
B								22
C								
N								
S			800					
F							67.6	
Cl							0.41	
Br								
Cu					6.4	4.5		
Zn							1.1(b)	
(ppb)								
I								
At								
Ga						5000		
Ge						84		
As								
Se								
Mo								
Tc								
Ru								
Rh								
Pd								
Ag								
Cd						16		
In						2.6		
Sn								
Sb								
Te								
Cs				480				
Ta				2150				
W								
Re								
Os								
Ir				43		0.14		
Pt								
Au				44		0.41		
Hg								
Tl								
Pb					1.91			
	(1)	(2)	(3)	(4)	(5)	(6)	(7)	(8)

splits. The consistent gamma ray data, which are for the total rock and also similar to those for 15206, suggest the A15 KREEP basalt is the dominant chemical component, consistent with most other analyses. Korotev's (1984 unpublished) data was determined on a small (less than ½ g) chip compared with that of Willis et al. (1972) (nearly 2 g). Willis et al. (1972) noted the high incompatible element abundances and the high SiO<sub>2</sub> content. The rare earth pattern is that of KREEP, and Reed and Jovanovic (1972) noted that halogens and other elements were strikingly similar to those in Apollo 14 soils. Schonfeld (1975) used a mixing model to infer 84 ± 2% of Apollo 15 KREEP basalt in 15205. Baedeker et al. (1973) used their data to infer a very low upper limit for siderophiles in A15 KREEP basalts, similar to mare basalts; they appear to be unaware of the mare basalts in 15205 in considering an origin for the rock as Imbrium ejecta.

Anderson and Hinthorne (1973) used an ion microprobe to determine the concentrations of Ba and rare earths in Y-Zr phosphate, whitlockite, and zircon, presumably derived from KREEP basalt clasts. These minerals have pronounced negative Eu anomalies and flat trivalent rare earth patterns.

STABLE ISOTOPES: Epstein and Taylor (1972) determined δO<sup>18</sup> values of 5.92 parts per mil and 6.07 parts per mil for gray matrix and black glass samples respectively. These are typical lunar values.

RADIOGENIC ISOTOPES AND GEOCHRONOLOGY: Anderson and Hinthorne (1973) used an ion microprobe to determine Pb isotopic ratios and Th/U ratios in zircon in 15205, determining an age of 4.01 ± 0.11 b.y. for the zircon. They did not specifically discuss the data.

RARE GASES, COSMOGENIC NUCLIDES, TRACKS, CRATERING, AND EXPOSURE: Drozd et al. (1976) made noble gas analyses of whole rock samples, primarily in pursuit of information on the excess xenon present in some lunar samples. They tabulated Kr and Xe isotopic data and tabulated summarized results. The excess xenon factor of 1.5 ± 0.2 is of low magnitude, easily understood in terms of in situ U and Pu decay. They determined an <sup>81</sup>Kr exposure age of 169 ± 7 m.y., which is rigorously an upper limit to the present configuration of the boulder. The high <sup>131</sup>Xe/<sup>126</sup>Xe and the long exposure suggest a complex, multistage exposure history, as also suggested by the much shorter track and microcratering ages (below).

Schaeffer et al. (1976) used a laser probe to analyze He, Ne, and Ar on exposed surfaces, comparing the spall zones of 100-micron craters with intercrater surfaces. Ne is of solar origin, but the irregular <sup>40</sup>Ar and high <sup>40</sup>Ar/<sup>36</sup>Ar (cf. solar) suggest a non-surface correlated origin for most <sup>40</sup>Ar. The two spall zones had 1/3 and 1/2 the "normal" content of all three gases, but one host had very low gases, possibly a result of a recent splash glass.

Keith et al. (1972) and Rancitelli et al. (1972) reported disintegration count data for cosmogenic radionuclides. They both found that <sup>22</sup>Na was at equilibrium but that <sup>26</sup>Al

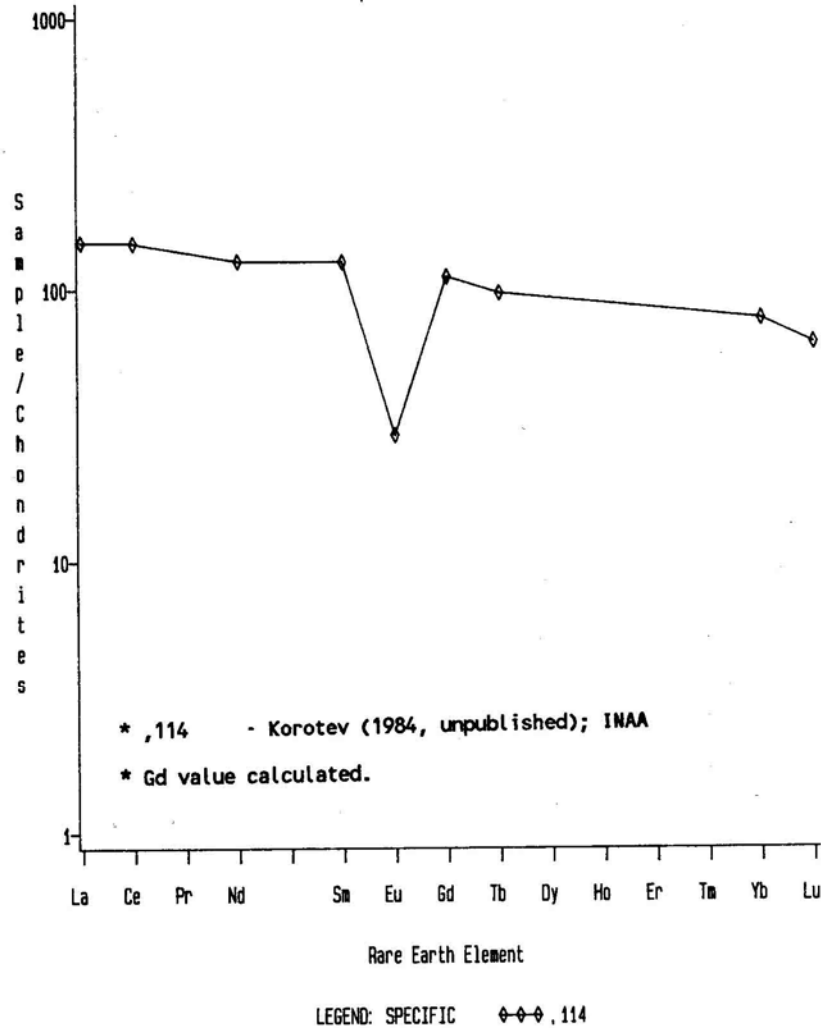


Figure 9. Rare earths in 15205 bulk rock (Korotev, 1984 unpublished).

was at one-half or one-third of saturation values, indicating a less-than-1-m.y. exposure. The low  $^{26}\text{Al}$  is not an artifact of composition (as confirmed by data for soil beneath the boulder and by the Yokoyama et al., 1974, analysis of the data). These cosmogenic nuclide data are similar to those for 15206. Fruchter et al. (1978) made new determinations and found  $^{26}\text{Al}$  to be 50% saturated and  $^{53}\text{Mn}$  to be 58% saturated, corresponding with exposure of  $0.7 \pm 0.1$  m.y. and  $4.5 \pm 0.5$  m.y. respectively. These ages are not consistent with each other nor with the Drozd et al. (1976) rare gas age, leading to the conclusion that 15205 was shielded at a depth of approximately 1 m for time period long with respect to the half-life of  $^{53}\text{Mn}$ . An exposure history consistent with  $^{26}\text{Al}$  age of 0.7 m.y.,  $^{53}\text{Mn}$  age of 4.5 m.y., and  $^{81}\text{Kr}$  age of 169 m.y. requires the boulder to have been buried just below the surface for 200 m.y., then ejected by a small event to its present position where it has remained for less than 100,000 years, consistent

with the solar flare track and microcrater ages (below). Bhandari (1977) also produced  $^{26}\text{Al}$  data for different depths (0-0.140 g/cm<sup>2</sup> and 1.5-1.64 g/cm<sup>2</sup>) for an exterior surface. He deduced an exposure age of less than or equal to 0.1 m.y., similar to other studies, from the unsaturated  $^{26}\text{Al}$ .

Schneider et al. (1973) derived a solar flare track age of about  $3 \times 10^4$  years, which was revised following new calibrations to  $7.9 \times 10^4$  years (Fechtig et al., 1974). These studies outline the depth dependence of solar flare tracks in the glass studied.

Schneider et al. (1973) reported cumulative crater number densities for a statistically significant number of craters (Fig. 10). The specimens were from the top corner of the boulder, and counting was done at several magnifications. The population is in production. The distribution is bimodal. These results have been discussed by Brownlee et al. (1973), Fechtig et al. (1974), and Horz et al. (1975, 1977) because of their implications for the micrometeoroid flux. Brownlee et al. (1973) noted that the bimodal distribution suggested two different source areas for micrometeoroid mass regimes. Hartung and Storzer (1974) continued the work with a study of the microcrater density and solar flare particle track exposure age measurements for the population, using iron-group solar flare tracks to yield exposure ages for host surface and 56 microcraters (Figs. 11, 12). They found individual microcrater exposure ages indicating an increasing microcrater production rate (flux) over the last 10,000 years (they suggested Comet Encke as the reason). This rate is higher than the present day production rate estimated from satellite and Apollo window data (Fig. 12), and Hartung and Storzer (1974) suspected that a systematic error existed in the analysis of solar flare particle tracks. However, this systematic error would not change the pattern of increasing micrometeoroid flux towards the present. According to Horz et al. (1975), the data for the last 3000 years are in good agreement with the present day flux. Zook et al. (1976) suggested that the Hartung and Storzer result should be inverted: probably solar activity fluctuates more.

PHYSICAL PROPERTIES: Adams and McCord (1972) measured the diffuse reflectance spectra (0.35 - 2.5 microns), and from the pyroxene bands deduced that 15205 had one of the least calcic pyroxenes among Apollo 15 rocks, which is in accordance with petrographic observations. Charette and Adams (1977) obtained similar spectra and distinguished the sample (although KREEP) from poikilitic (= low-K Fra Mauro, Apollo 16, 17) rocks on spectral characteristics.

PROCESSING AND SUBDIVISIONS: A small chip (,2) was knocked off (location uncertain) and was used to make thin sections ,3 through ,7. Subsequently the rock was sawn parallel to two faces and the slabs (which have exterior glass) further dissected (Fig. 13). Most allocations have been made from these subdivisions. In 1977 ,0 was further subdivided to produce a few small pieces (,96 - ,102, total less than 15 g) (e.g., Fig. 1c) so that interior pieces could be obtained. One chip was partly used to make thin section ,122. A small chip of glass coat was also removed to make thin section ,110. ,0 is now 139.8 g; no other pieces larger than 25 g exist.

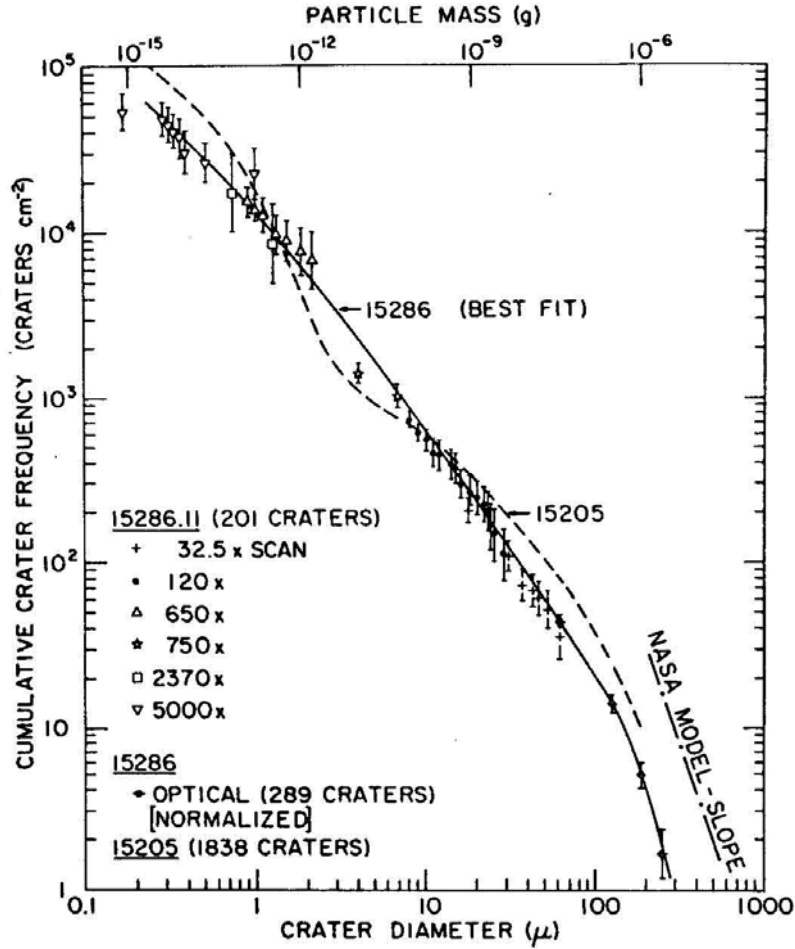


Figure 10. Size frequency data for microcraters on 15205 and for 15286 (15205 data from Schneider et al., 1973; diagram from Brownlee et al., 1973).

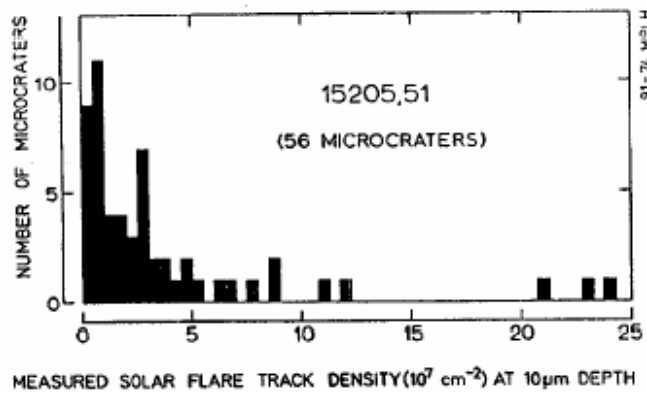


Figure 11. Distribution of microcraters according to measured solar flare track density at a depth of about 10 microns below the surface of a microcrater pit (Hartung and Storzer, 1974)

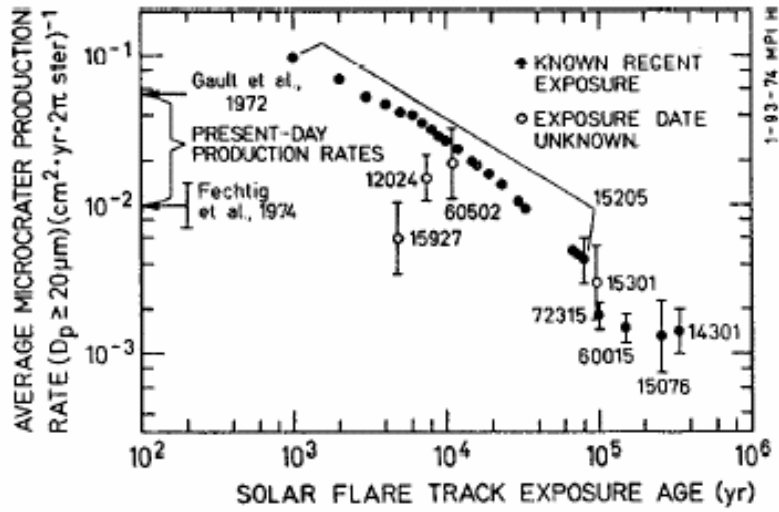


Figure 12. Exposure age data for individual microcraters on 15205 indicating a decreasing average microcrater production rate with time in the past (Hartung and Storzer, 1974).

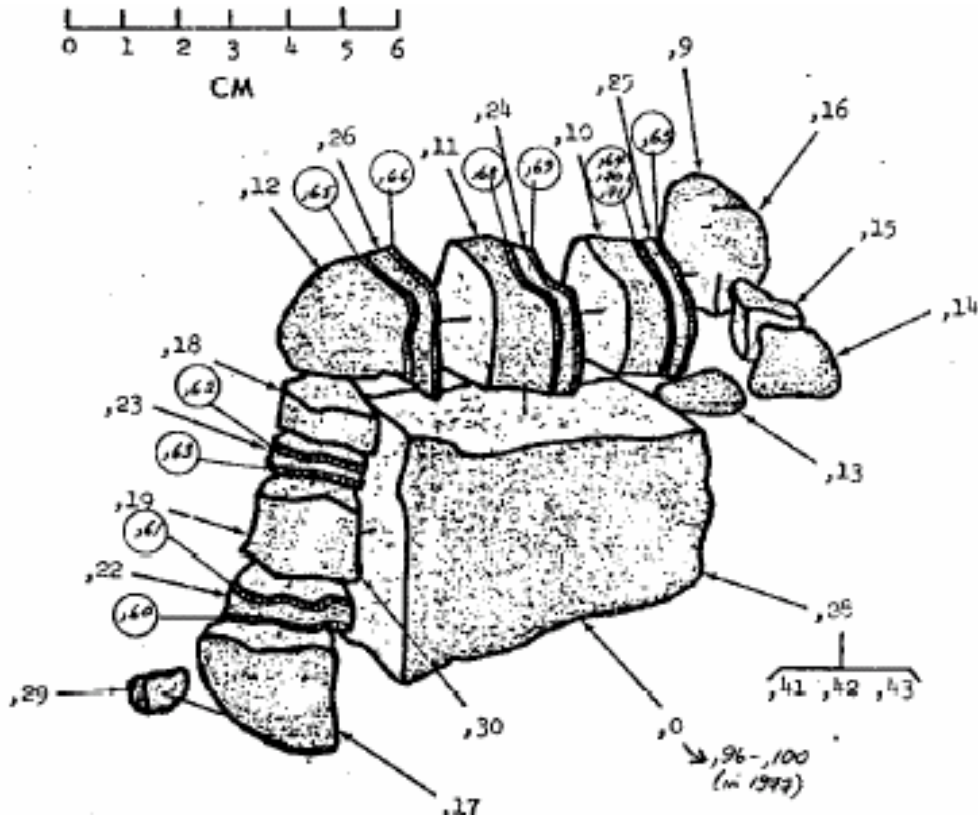


Figure 13. Sawing of 15205 into slabets, 1972. Circled numbers show

locations of thin sections cut from these slablets. Other thin sections were also cut.